The Ndc80 internal loop is required for recruitment of the Ska complex to establish end-on microtubule attachment to kinetochores

Gang Zhang[1,2], Christian D. Kelstrup[1], Xiao-Wen Hu[3], Mathilde J. Kaas Hansen[2], Martin R. Singleton[3], Jesper V. Olsen[1] and Jakob Nilsson[1,2,*]

[1]The Novo Nordisk Foundation Center for Protein Research, Faculty of Health Sciences, University of Copenhagen, Blegdamsvej 3b, 2200 Copenhagen, Denmark
[2]BRIC, University of Copenhagen, Ole Maaløes Vej 5, 2200 Copenhagen, Denmark
[3]CRUK, London Research Institute, 44 Lincoln's Inn Fields, London WC2A 3LY, UK
*Author for correspondence (jakob.nilsson@cpr.ku.dk)

Accepted 20 February 2012
Journal of Cell Science 125, 3243–3253

doi: 10.1242/jcs.104208

Summary

The Ndc80 complex establishes end-on attachment of kinetochores to microtubules, which is essential for chromosome segregation. The Ndc80 subunit is characterized by an N-terminal region that binds directly to microtubules, and a long coiled-coil region that interacts with Nuf2. A loop region in Ndc80 that generates a kink in the structure disrupts the long coiled-coil region but the exact function of this loop, has until now, not been clear. Here we show that this loop region is essential for end-on attachment of kinetochores to microtubules in human cells. Cells expressing loop mutants of Ndc80 are unable to align the chromosomes, and stable kinetochore fibers are absent. Through quantitative mass spectrometry and immunofluorescence we found that the binding of the spindle and kinetochore associated (Ska) complex depends on the loop region, explaining why end-on attachment is defective. This underscores the importance of the Ndc80 loop region in coordinating chromosome segregation through the recruitment of specific proteins to the kinetochore.

Key words: Ndc80 complex, Ska complex, Kinetochore

Introduction

The kinetochore is the macromolecular structure responsible for aligning and segregating sister chromatids during mitosis and for establishing the 'wait anaphase signal' of the spindle assembly checkpoint (SAC) (Cheeseman and Desai, 2008; Welburn and Cheeseman, 2008). It assembles on the centromere region and is able to stably attach to dynamic microtubules a property required for faithful chromosome segregation. The kinetochore is composed of approximately 80 proteins present in multiple copies and a sub-complex referred to as the KMN network (KNL1–Mis12–Ndc80 network) is able to bind directly to microtubules (Cheeseman et al., 2006). Within the KMN network the Ndc80 complex, composed of Ndc80, Nuf2, Spc24 and Spc25 plays an important role in binding to microtubules (DeLuca et al., 2002; Martin-Lluesma et al., 2002; Wigge and Kilmartin, 2001) via the calponin homology domains (CHDs) of Ndc80 and Nuf2 and the unstructured N-terminal tail of Ndc80 (Alushin et al., 2010; Ciferri et al., 2008; DeLuca et al., 2005; DeLuca et al., 2006; Guimaraes et al., 2008; Miller et al., 2008; Powers et al., 2009; Sundin et al., 2011; Tooley et al., 2011). The binding of the Ndc80 complex to microtubules is negatively regulated by the error correction machinery through the direct phosphorylation of residues in the N-terminal tail of the Ndc80 subunit by Aurora B (Akiyoshi et al., 2009; DeLuca et al., 2006; Welburn et al., 2010). In addition the KNL1 subunit of the KMN network has microtubule binding activity and both the Ndc80 complex and KNL1 contributes to the overall microtubule binding activity of the kinetochore (Cheeseman et al., 2006).

The Ndc80 complex is an elongated rod-like molecule of approximately 55 nm composed of a central long coiled-coil region and terminal globular domains (Ciferri et al., 2005; Ciferri et al., 2008; Wei et al., 2005). Architecturally the Ndc80 complex is composed of the Ndc80–Nuf2 dimer the C-terminus of which binds the N-terminus of the Spc24–Spc25 dimer. The Spc24–Spc25 globular domains tether the complex to the inner kinetochore allowing the microtubule binding activity of Ndc80 to face outwards from the kinetochore. The long coiled-coil region of Ndc80 is disrupted by a loop region, which potentially results in a kink in the structure as revealed by electron microscopy (EM) analysis (Wang et al., 2008). Although the loop is only weakly conserved in sequence its position in the coiled-coil is conserved. The exact function of this internal loop region is not clear but it has recently been shown to be essential for end-on attachment and microtubule dynamics in both *Saccharomyces cerevisiae* and *Schizosaccharomyces pombe* through the recruitment of the Dam1 complex or Dis1 respectively (Hsu and Toda, 2011; Maure et al., 2011; Schmidt and Cheeseman, 2011). In mammalian cells it has been proposed to be part of an intra-kinetochore tension sensor based on careful measurements of kinetochore protein distances (Wan et al., 2009). Although the loop likely gives rise to flexibility in the Ndc80 complex, the projection distance along the inter-kinetochore axis does not change (Wan et al., 2009).

Journal of Cell Science

Although the KMN network constitutes the main microtubule binding activity of the kinetochore a range of proteins play a role at the interface of microtubules and the kinetochore ensuring proper attachment. This includes the spindle and kinetochore-associated (Ska) complex (Daum et al., 2009; Gaitanos et al., 2009; Hanisch et al., 2006; Theis et al., 2009; Welburn et al., 2009), the checkpoint proteins Bub1 (Meraldi and Sorger, 2005) and BubR1 (Lampson and Kapoor, 2005), Cenp-E (Yen et al.,

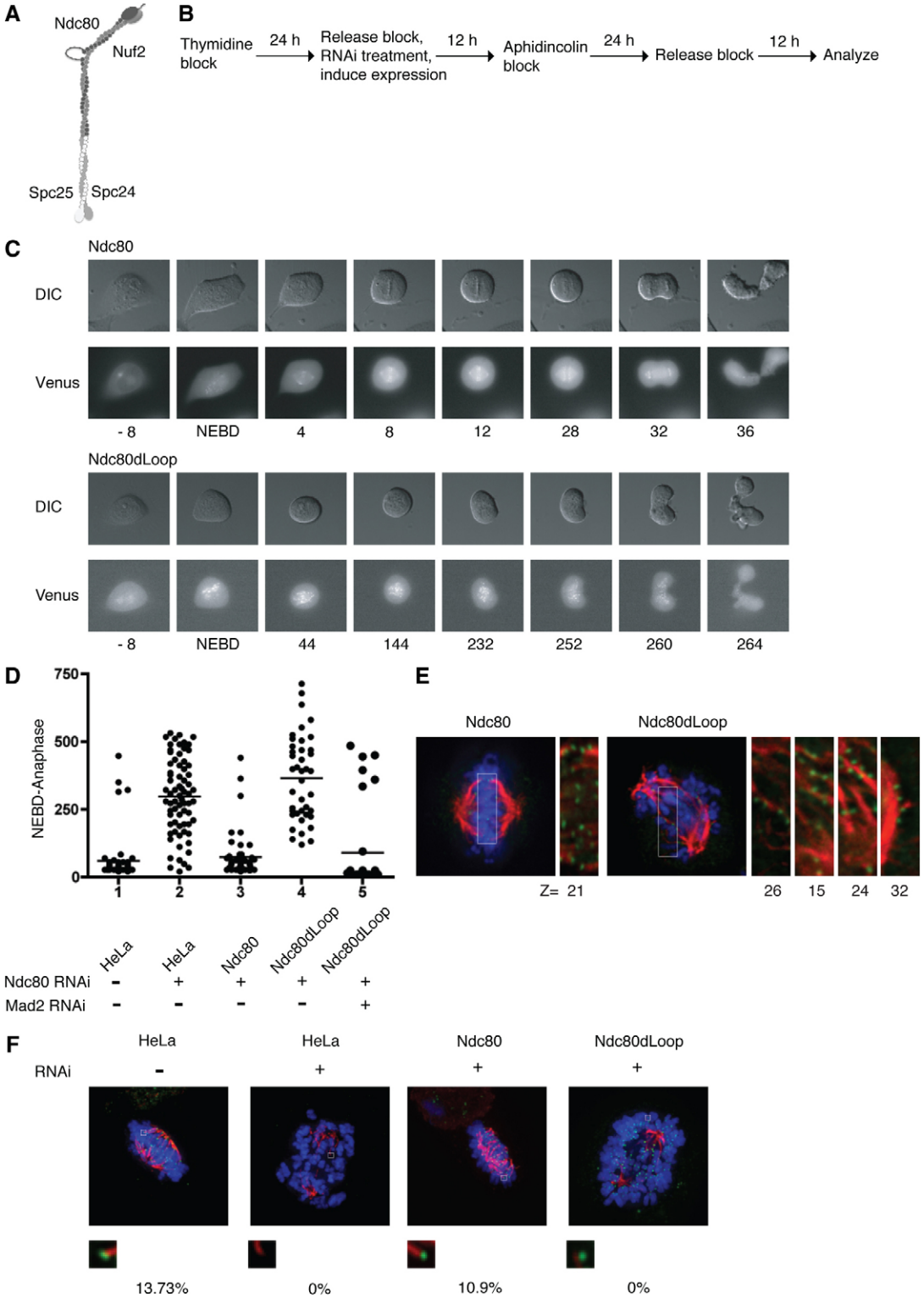

Fig. 1. See next page for legend.

1991), Dynein–Dynactin (Whyte et al., 2008), the RZZ complex (Karess, 2005), Spindly (Barisic et al., 2010; Chan et al., 2009) and the Astrin–Skap complex (Schmidt et al., 2010) as well as a range of microtubule plus-end directed motor proteins. Exactly how microtubule binding by the KMN network is integrated with the activities of these proteins is a significant question.

Here we have investigated the role of the internal loop region of human Ndc80. We find that the loop is essential for establishing end-on attachments to microtubules by regulating the recruitment of the Ska complex to kinetochores.

Results

The Ndc80 internal loop is essential for end-on microtubule attachment

A coiled-coil prediction of human Ndc80 reveals that the region from amino acid 426 to 459 disrupts the coiled-coil structure potentially forming a loop region (Fig. 1A; supplementary material Fig. S1A). To analyze the role of this loop region in Ndc80 we first established a system to remove the endogenous Ndc80 using RNAi and then express siRNA resistant versions of Ndc80 tagged with the YFP variant Venus at the C-terminus. Inducible isogenic HeLa cell lines were generated using the FRT system allowing comparison of wild-type Ndc80 and mutant versions. Recording both differential interference contrast (DIC) images and the Venus signal by time-lapse microscopy allowed us to analyze mitotic defects (Fig. 1). Upon depletion of Ndc80 the cells mounted a robust mitotic arrest and chromosomes never formed a metaphase plate as expected. Although the depletion of Ndc80 was efficient residual amounts remained sufficient to activate the SAC (Meraldi et al., 2004). The induction of wild type Ndc80 resulted in complete rescue of this phenotype as cells aligned and segregated their chromosomes with normal kinetics showing that our complementation assay worked (Fig. 1C,D). In contrast cells expressing a version of Ndc80 with most of the loop region removed, Ndc80 (Δ427–452) (hereafter referred to as Ndc80dLoop), were unable to rescue the Ndc80 RNAi phenotype and the chromosomes never managed to form a metaphase plate resulting in a Mad2 dependent arrest (Fig. 1C,D). Cells depleted of Ndc80 or expressing Ndc80dLoop rarely entered anaphase and most cells stayed arrested throughout the recording and 'anaphase' was set to the time the recording ended, which underestimates the NEBD–anaphase transition under these conditions. The Ndc80dLoop construct appeared to localize to kinetochores normally as judged by the dot like appearance of the Venus signal. The same phenotype was observed in cells expressing Ndc80dLoop without depletion of the endogenous Ndc80, showing that Ndc80dLoop phenotype is dominant (supplementary material Fig. S2). This revealed that the loop region of Ndc80 is essential for chromosome alignment and segregation.

To analyze the defects in Ndc80dLoop expressing cells in more detail we performed immunofluorescence analysis staining for microtubules and Ndc80. In agreement with the live cell analysis, cells rescued with Ndc80 formed metaphase plates with microtubules making end-on attachment to kinetochores (Fig. 1E). Cells rescued with Ndc80dLoop did not form a metaphase plate but lateral interactions with microtubules were observed when single z-sections were inspected (Fig. 1E). These observations were further confirmed by performing a cold-stability assay (Rieder, 1981; Salmon and Begg, 1980), which only allows stable kinetochore microtubules (K-fibers) to remain. In Ndc80 depleted cells cold-stable K-fibers were completely absent but expression of Ndc80 rescued this and restored the number of cells displaying a metaphase configuration to control levels (Fig. 1F). In contrast the rescue with Ndc80dLoop did not restore K-fibers and cells with a metaphase plate configuration were absent.

Together these results show that the loop region of Ndc80 is essential for end-on microtubule attachment in human cells.

Fig. 1. The Ndc80 internal loop region is essential for end-on attachment to microtubules. (**A**) Schematic of the Ndc80 complex. (**B**) Protocol used for synchronization and RNAi of Ndc80 and rescue with either Ndc80 or Ndc80dLoop. (**C**) Ndc80 was depleted by RNAi in HeLa cell lines stably expressing inducible RNAi-resistant versions of Ndc80 or Ndc80dLoop tagged with Venus at the C-terminus. The cells were filmed and the DIC images and Venus signal were recorded to monitor progression through mitosis. Time in minutes from nuclear envelope breakdown (NEBD) is indicated below the frames. (**D**) Distribution of NEBD–anaphase in control cells ($n=64$), cells depleted of Ndc80 ($n=73$), cells rescued with either Ndc80 ($n=53$) or Ndc80dLoop ($n=41$) in the presence or absence of Mad2 ($n=33$). Each dot represents a single cell analyzed. The time from NEBD–anaphase in Ndc80 RNAi and in cells expressing Ndc80dLoop is underestimated as cells normally stayed arrested for the duration of the recording and therefore never entered anaphase. However, anaphase was set to the end of recording for cells that had been monitored for at least 2 hrs. (**E**) Immunofluorescence analysis of cells depleted of endogenous Ndc80 and rescued with Ndc80 or Ndc80dLoop and stained for Ndc80 (green), microtubules (red) and chromosomes (blue). The higher magnification images of the boxed areas (to the right of each main image) are from single z-sections and show the lateral attachments that Ndc80dLoop makes to microtubules. Several z-sections are shown for Ndc80dLoop whereas one is shown for Ndc80. (**F**) Cells were incubated for 15 min on ice before fixation and staining for Ndc80 (green) and microtubules (red). 200 mitotic cells were inspected for each condition, and number of cells in metaphase and that were displaying cold-stable microtubules were scored (number indicated below the still images). The enlarged area (below) shows the absence of end-on attachment in cells rescued with Ndc80dLoop.

The internal loop region is not required for forming a proper Ndc80 complex

Although the Ndc80dLoop appeared to localize normally to kinetochores the observed defects in end-on attachment could be the result of improper Ndc80 complex formation. To address this we first reconstituted the Ndc80 and Ndc80dLoop complexes from purified components expressed in bacteria and analyzed the complexes by size-exclusion chromatography on a Superose 6 column. The two eluted at the expected size (Ciferri et al., 2005) with similar stoichiometry of the four subunits (Fig. 2A,B). In all our purifications the Ndc80dLoop complex migrated slightly slower on the size exclusion column indicating a change in Stokes radius. We used the purified complexes in microtubule pelleting assays to assess their microtubule binding ability. A precise comparison was complicated by the fact that the Ndc80dLoop complex was able to pellet a small amount in the absence of microtubules. Taking the amount of Ndc80 complexes pelleting in the absence of microtubules into account we did not observed a major difference in binding (Fig. 2B,C). This is to be expected as the microtubule binding activity of the Ndc80 complex resides in the N-terminus of the Ndc80–Nuf2 dimer and in line with the observation that the Ndc80 bonsai construct binds normally to microtubules (Ciferri et al., 2008).

Finally we analyzed the complexes by electron microscopy (EM) and negative stain to determine if removal of the loop

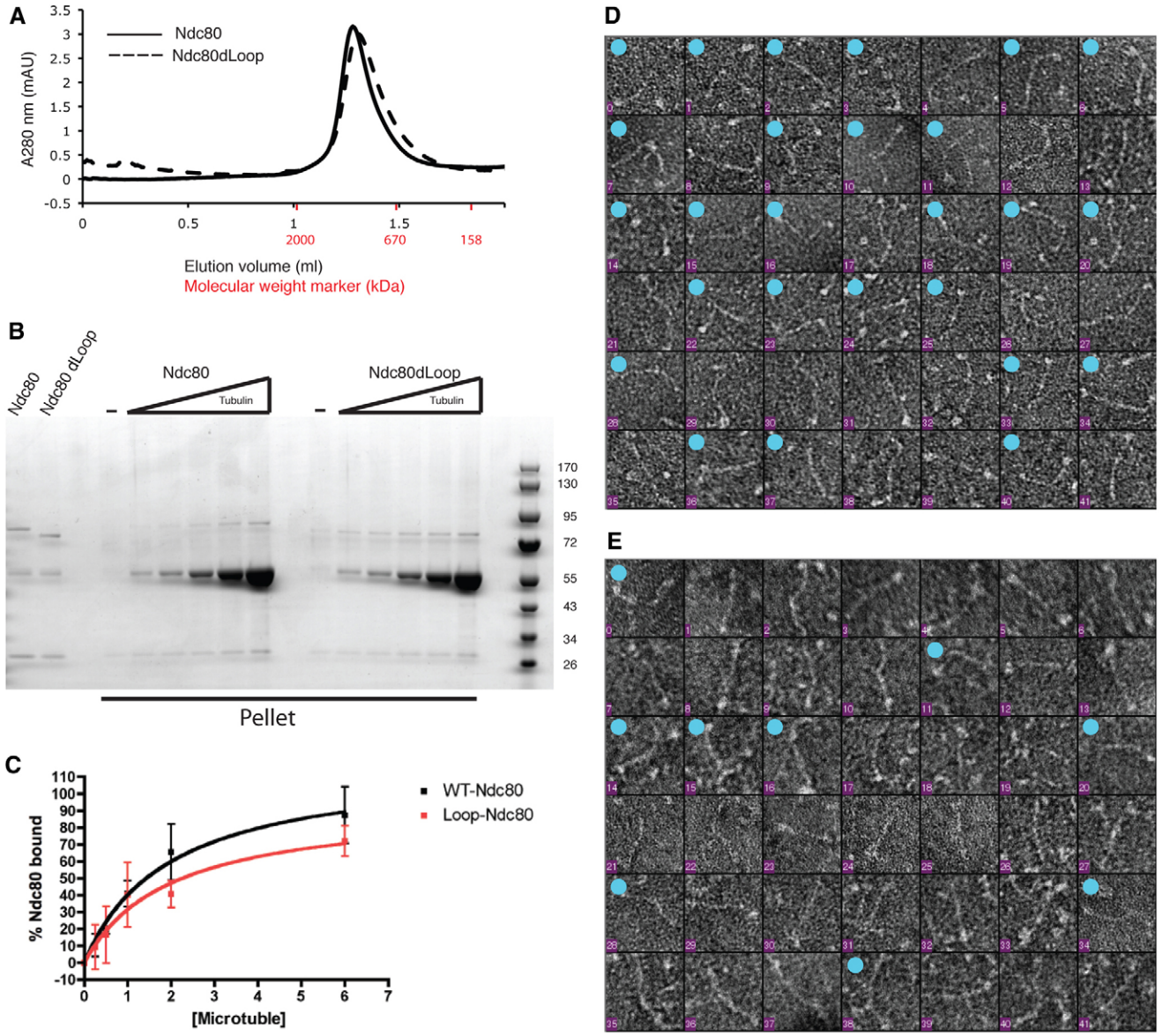

Fig. 2. The Ndc80 complex can form in the absence of the loop region. (**A**) Purified reconstituted Ndc80 and Ndc80dLoop complexes were analyzed on a Superose 6 column and their elution profile is displayed. Ndc80 and Ndc80dLoop complexes both eluted at approximately 700 kDa. (**B**) Microtubule pelleting assay using purified Ndc80 and Ndc80dLoop complexes. 0.2 μM Ndc80 complex was incubated with 0, 0.25, 0.5, 1, 2 or 6 μM-Taxol stabilized microtubules and incubated for 5 minutes at room temperature. The reaction was placed on a glycerol cushion and microtubules were pelleted. The pellet was dissolved and analyzed by SDS-PAGE and Coomassie Blue staining. (**C**) Quantification of the microtubule pelleting assay from two independent experiments. The intensity of the Ndc80 band from the Coomassie-stained gel was quantified and the amount of Ndc80 pelleting in the absence of microtubules was subtracted. The maximum amount of Ndc80 complex able to bind was based on the input and set to 100%. The values were fitted to a one-site binding model and the mean and standard deviation is shown. (**D**) Electron micrograph of 42 particles of reconstituted Ndc80 complexes. Ndc80 molecules can be clearly distinguished and molecules containing a prominent kink, two-thirds of the distance along the molecule, are indicated with a blue dot. (**E**) Electron micrograph of 42 particles of reconstituted Ndc80dLoop complexes, with a blue dot indicating the complexes with a kink.

affected the structure of the Ndc80 complex. We analyzed 42 molecules of Ndc80 complexes and scored whether they displayed the very characteristic kink that has been observed (Wang et al., 2008). As the Ndc80 complexes show a distribution of angles this is a slightly arbitrary scoring but it did reveal that approximately 60% (26 out of 42) of Ndc80 complexes displayed the kink in agreement with a previous study (Fig. 2D) (Wang et al., 2008). The analysis of Ndc80dLoop complexes by EM was complicated by the fact that the molecules seemed to cluster on the grids and fewer single molecules were clearly visible. We did identify 42 single molecules of the Ndc80dLoop complexes and analysis of these complexes revealed that only 9 molecules out of these displayed the kink. Using this classification, a Fisher exact test (two-tailed) gives a *P*-value of 0.0003, showing that there is a correlation between the presence of the loop, and degree of kinking in the particle.

Overall our biochemical analysis supports that the Ndc80 complex can assemble properly in the absence of the loop region and that defects in assembly and microtubule binding is not the likely cause of the observed phenotype. We cannot rule out the possibility that in the context of the kinetochore the exact orientation of the microtubule binding activity of Ndc80 is critical for microtubule binding.

An artificial loop sequence results in a similar phenotype as Ndc80dLoop

The EM analysis pointed towards structural changes in the Ndc80dLoop complex which was to be expected as the loop region is likely responsible for creating the kink in the structure. To determine whether a structural change in Ndc80 could account for the defect in end-on attachment we reversed the amino acid sequence from 427–450, which created an Ndc80 molecule with the same coiled-coil prediction as Ndc80 but with a loop sequence with no sequence similarity to the original sequence (Fig. 3A; supplementary material Fig. S1). This form of Ndc80 will be referred to as Ndc80rLoop. We created an isogenic stable HeLa cell line expressing Ndc80rLoop–Venus and performed RNAi-rescue experiments and analyzed this both by time-lapse microscopy and immunofluorescence. Ndc80rLoop had a phenotype very similar to Ndc80dLoop in that cells did not form a metaphase plate and arrested in mitosis for a prolonged time (Fig. 3B). Similarly there were no cold-stable K-fibers present in these cells again indicating a failure in end-on microtubule attachment (Fig. 3C).

This result shows that an artificial loop is not able to support the function of the loop region potentially indicating that the exact sequence of the loop is important. Whether the artificial loop alters the flexibility of the Ndc80 complex and this is the reason why the Ndc80rLoop is not functional is currently not clear.

Quantitative mass spectrometry reveals the absence of the Ska-complex in Ndc80dLoop complexes purified from cells

Our results with the Ndc80rLoop indicated to us that maybe the loop region of Ndc80 was interacting with proteins required for kinetochore microtubule interactions in line with the recent observations in yeast.

To determine which proteins depended on the loop region for interaction with Ndc80 we employed a quantitative mass spectrometry approach (Ong et al., 2002; Ong and Mann, 2006) in which cell lines were isotopically labeled resulting in three distinct cell populations that could be simultaneously analyzed in the mass spectrometer (Fig. 4A). Briefly, stable isotope labeling of amino acids in cell culture (SILAC) was employed. The parental HeLa cell line was labeled with amino acids to give rise to the light condition (L), Ndc80–Venus expressing cells labeled to give rise to the medium condition (M) and Ndc80dLoop–Venus expressing cells labeled to give the heavy condition (H).

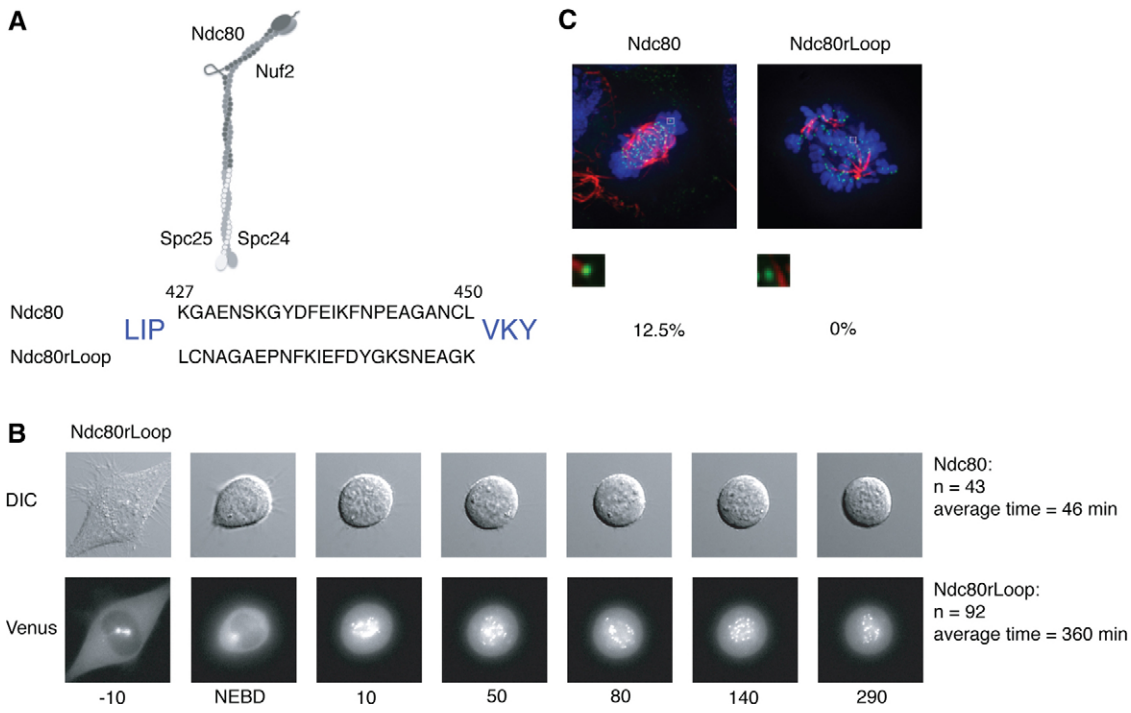

Fig. 3. The sequence of the loop region is important for end-on attachment. (**A**) Schematic of the Ndc80rLoop version of Ndc80. The sequence of the loop in Ndc80 is compared to that of Ndc80rLoop. (**B**) Endogenous Ndc80 was depleted by RNAi and then rescued with either Ndc80 or Ndc80rLoop and the DIC images and Venus signal were recorded. The time (in minutes) from NEBD is given under each frame. Only Ndc80rLoop images are shown. In total, 43 cells were analyzed for the Ndc80 rescue and 92 cells analyzed for the Ndc80rLoop rescue. The average time from NEBD–anaphase is indicated on the right. The cells expressing Ndc80rLoop were arrested throughout the recordings, and anaphase was set to the end of recordings, which underestimates the average time. (**C**) Cells rescued with either Ndc80 or Ndc80rLoop were treated for 15 minutes on ice before fixation and staining for microtubules (red) and Ndc80 (green). 200 mitotic cells were analyzed for each condition and scored for the presence of cold-stable K-fibers and a metaphase configuration of chromosomes. The percentages of cells with a metaphase plate and cold stable microtubules is indicated below the images.

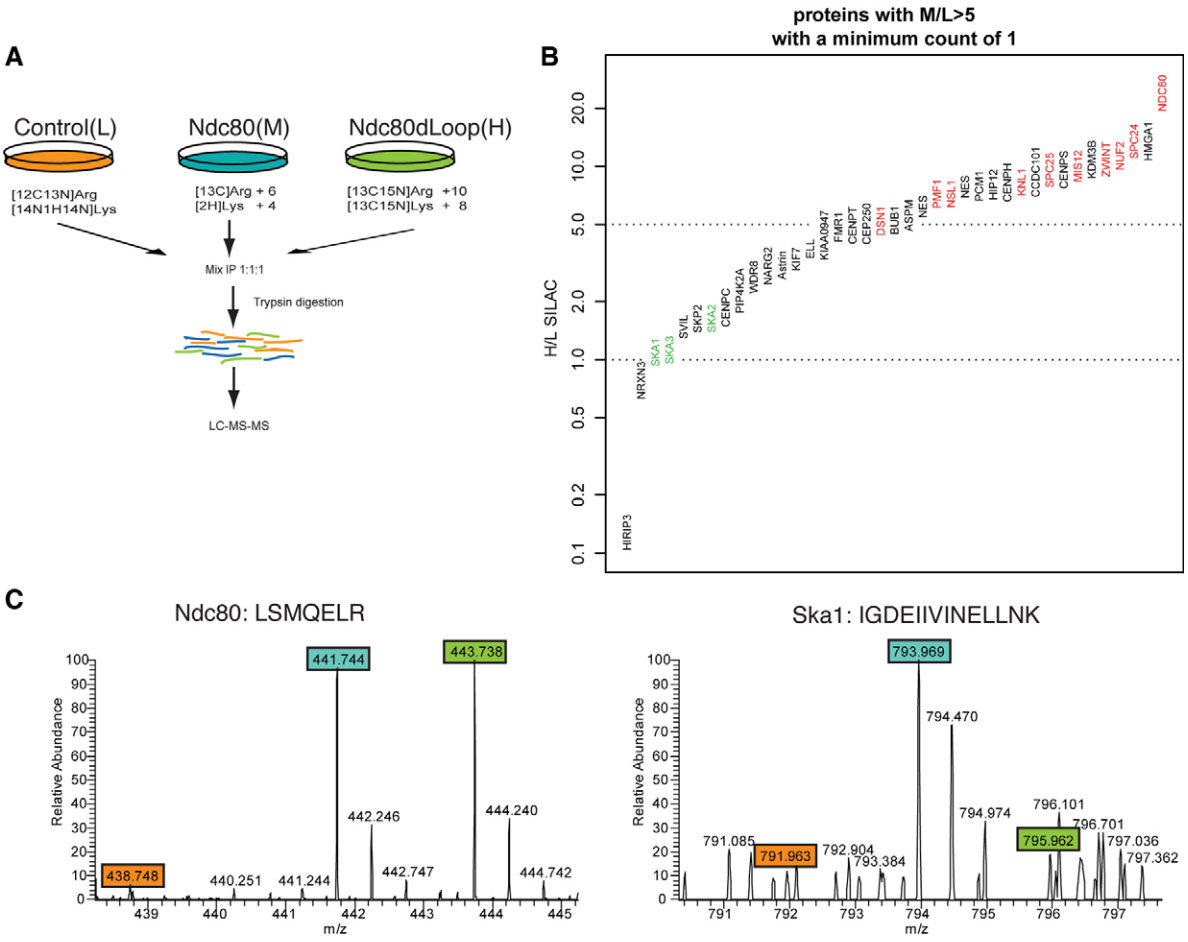

Fig. 4. The Ska complex is absent from Ndc80dLoop purifications. (**A**) Schematic of the SILAC approach used to identify specific interactors of the Ndc80 loop region. Three cell populations were labeled with different isotopes as indicated to produce a light (L), a medium (M) and a heavy (H) cell population that could be distinguished in the mass spectrometer. The light sample was a control purification whereas the medium sample expressed Ndc80–Venus and the heavy sample expressed Ndc80dLoop–Venus. Following purification with GFP binder the samples were mixed 1:1:1 and analyzed by LC–MS. (**B**) Plot of H/L ratios from the Ndc80dLoop sample for the subset of proteins in the Ndc80 sample that had a M/L ratio of ~5. Red indicates the KMN network components and green indicates the three Ska complex components. Two peptides were detected for Ska1 and three peptides for Ska2. For Ska3 we only detected 1 peptide. (**C**) Examples of recorded spectra for an Ndc80 peptide and a peptide of Ska1. The color scheme is the same as in A. The mass to charge value is indicated above each peak.

Cells were arrested in prometaphase with nocodazole and harvested by mitotic shake-off and Ndc80 complexes purified under mild conditions using GFP-binder (Rothbauer et al., 2008). We chose to arrest cells with nocodazole because the Ndc80dLoop expressing cells were not able to make end-on attachment to microtubules and therefore a quantitative comparison would be complicated by the difference in microtubule binding between the Ndc80 and Ndc80dLoop complexes. Adding nocodazole prevented this problem as microtubules are removed. The purified complexes were eluted and the eluates were mixed 1:1:1 and analyzed simultaneously by mass spectrometry. Ndc80 and Ndc80dLoop displayed similar ratios and co-purified all components of the KMN network as well as a number of CENP proteins (Fig. 4B). There was a reduction in the H/L ratio of all KMN network components in the Ndc80dLoop sample compared to the M/L ratio observed in Ndc80 sample and the ratio of Cenp-C was very low in the Ndc80dLoop sample. This either indicates a less stable KMN network with components being lost during purification or less efficient incorporation into the kinetochore of Ndc80dLoop. We also identified all three components of the Ska complex in Ndc80 purifications with high ratios but low intensity. Importantly all three Ska complex components were strongly reduced in Ndc80dLoop purifications showing peptide ratios similar to the control purifications (Fig. 4B,C). This was not a general trait of dynamic kinetochore proteins such as Bub1, BubR1 and Astrin as they were still present although reduced in Ndc80dLoop purifications (Fig. 4B, and data not shown).

Our mass spectrometry analysis revealed that binding of the Ska complex was extremely sensitive to the removal of the internal loop region indicating that the Ska complex could make a direct interaction with this region. Since the complex purifications were done from nocodazole-arrested cells and at low temperature the interaction we observe with the Ska complex is unlikely to be mediated by microtubules.

Recruitment of the Ska complex to the kinetochore requires the internal loop region of Ndc80

It has previously been shown that the recruitment of the Ska complex to kinetochores depends on Ndc80 (Hanisch et al., 2006).

To further explore the role of the internal loop region of Ndc80 in recruitment of the Ska complex we removed the endogenous Ndc80 and rescued with either wild type Ndc80 or loop mutants. In our analysis we included a version of Ndc80 with a mutation in the toe region, Ndc80 K166E, which is known to disrupt microtubule binding (Alushin et al., 2010; Tooley et al., 2011). Indeed our characterization of Ndc80 K166E revealed a failure of cells to form cold-stable microtubules and cells displayed a prolonged mitotic arrest similar to Ndc80 loop mutants (supplementary material Fig. S3). Since the recruitment of the Ska complex to the kinetochore is sensitive to microtubule binding including Ndc80 K166E in the analysis allowed us to discriminate between general defects due to a failure in microtubule binding and specific defects due to the removal of the loop region.

To analyze the effect of Ndc80 mutants on kinetochore localization of the Ska complex we performed RNAi rescue experiments with the different forms of Ndc80. The Ska3 signal on kinetochores was quantified from cells in prometaphase during an unperturbed mitosis and normalized to the CREST signal. We also stained for Ndc80 in the same cells to ensure the RNAi rescue had worked and that Ndc80 was incorporated. We did not see any differences in Ndc80 levels in these experiments indicating full incorporation of the different forms (see Fig. 6B).

Removal of Ndc80 by RNAi resulted in the loss of Ska3 staining from the kinetochore and this was restored to normal levels by expressing wild type Ndc80 (Fig. 5A,B). Expression of Ndc80 K166E restored the levels of Ska3 at kinetochores to approximately 90% of its normal levels. In contrast, Ndc80dLoop and Ndc80rLoop restored Ska3 staining at kinetochores to approximately 20% and 40% respectively. Similar observations were obtained with an antibody towards the Ska1 component (supplementary material Fig. S4) but the staining with this antibody had a higher background than the Ska3 antibody.

This analysis reveals a role of the Ndc80 loop region in recruiting the Ska complex to kinetochores.

A fraction of KNL1 is specifically reduced at the kinetochore in Ndc80 loop mutants

The mass spectrometry analysis indicated that KMN network components co-purified less efficiently with Ndc80dLoop and therefore we investigated their kinetochore localization carefully by quantitative immunofluorescence in Ndc80 loop mutants.

To analyze the assembly of the KMN network and other components of the kinetochore we performed an RNAi rescue experiment with Ndc80 and Ndc80dLoop and stained for kinetochore components in nocodazole treated cells. As expected the removal of Ndc80 resulted in greatly reduced levels of Spc25 on the kinetochores and the localization of Spc25 was restored to equal levels upon expression of both Ndc80 and Ndc80dLoop (Fig. 6). Although the staining of our Nuf2 antibody was not sufficiently good to allow a quantitative comparison there appeared to be equal levels at kinetochores in Ndc80 and Ndc80dLoop (data not shown). Zwint and CENP-H levels, components of the KMN and CCAN network respectively, were partly reduced in their levels and this was also restored upon expression of both forms of Ndc80. Kinetochore localization of the Mis12 complex component DSN1 was not affected by the removal of Ndc80. The SAC protein Mad1 was also present at normal levels indirectly supporting that the RZZ complex was recruited to Ndc80dLoop (data not shown).

In contrast when we analyzed the localization of KNL1 this was reduced by the removal of Ndc80 to approximately 70% of its levels in control cells. Although rescue with Ndc80 restored the levels of KNL1 at the kinetochore this was not the case for either Ndc80dLoop or Ndc80rLoop (supplementary material Fig. S5). To determine whether this effect was specific to the Ndc80 loop mutants we also included Ndc80 K166E in the analysis. In the kinetochores containing Ndc80 K166E the levels of KNL1 was almost restored to that observed in kinetochores incorporating wild type Ndc80, indicating that the reduction of KNL1 is specific to the loop mutants.

We conclude from these observations that a fraction of KNL1 depends on Ndc80 for incorporation into the kinetochore and that this incorporation requires the loop region of Ndc80 (supplementary material Fig. S5).

Discussion

The loop region as a flexible scaffold for recruiting proteins to the Ndc80 complex

Our analysis reveals that the internal loop region of human Ndc80 is essential for kinetochores to make end-on attachment to microtubules. There are likely several factors contributing to this namely a potential change in the orientation of the N-terminus of Ndc80 with respect to other KMN network components and also a failure in recruitment of the Ska complex. Interestingly recent studies in fungi have also shown that the loop region regulates kinetochore microtubule dynamics and end-on attachment through the recruitment of Dis1 or the Dam1 complex (Hsu and Toda, 2011; Maure et al., 2011). The internal loop region thus has a conserved function in recruiting specific factors to the kinetochore. The Ska complex has been proposed to be the functional equivalent of the yeast Dam1 complex and it is interesting to note that both complexes appear to be dependent on the loop region. Since a loop region allows great sequence flexibility it can easily adapt to recruit specific proteins in different species while still maintaining the kink in the Ndc80 structure. The position of the loop approximately 20 nm away from the microtubule binding activity of the Ndc80/Nuf2 heads (Wang et al., 2008) is also close enough to influence the microtubule binding activity of the kinetochore (supplementary material Fig. S6). Furthermore, since the plus ends of microtubules are found approximately 10–15 nm inside the Spc24/25 heads (Wan et al., 2009) proteins bound to the loop would also be close to the dynamic microtubule termini.

In addition to providing a binding site for more dynamic kinetochore proteins we also find that the loop region in human cells has an impact on KNL1 levels. In our hands depletion of Ndc80 results in reduction of KNL1 levels by 30% (in some experiments up to 40%), which was not restored by expression of either Ndc80 loop mutants. Whether this reflects an outright interaction of the Ndc80 complex with KNL1 or is due to the loss of the Ska complex, the depletion of which also reduces KNL1 levels (Gaitanos et al., 2009), is not clear. We note that no direct binding between Ndc80 and KNL1 has been observed in studies where this was investigated (Maskell et al., 2010; Petrovic et al., 2010). Given that the entire KMN network seems less stable in Ndc80dLoop complexes based on the observed reduction in co-purifying KMN network components identified by mass spectrometry, it could be that the loop assists in stabilizing the entire KMN network or that a change in Ndc80 structure upon removal of the loop affects KMN network stability.

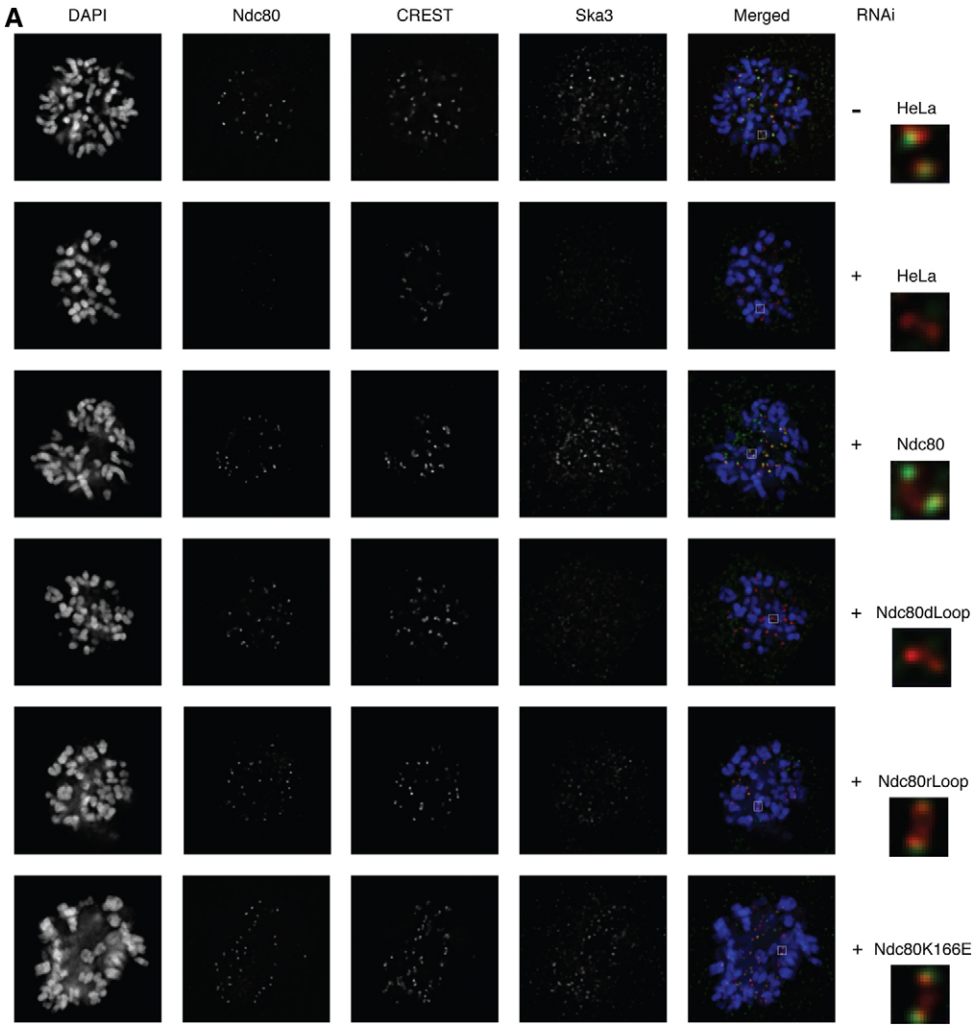

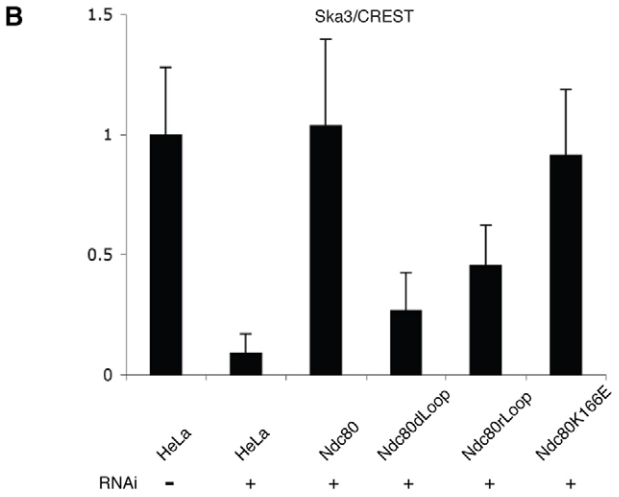

Fig. 5. Localization of the Ska complex to kinetochores requires the internal loop region of Ndc80. (**A**) Immunofluorescence analysis of Ska3 localization to kinetochores following the depletion of Ndc80 and rescue with the indicated Ndc80 forms. Cells in prometaphase during an unperturbed mitosis were analyzed and stained for Ndc80, Ska3 and CREST. The merged images are of the DAPI signal (blue), CREST signal (red) and the Ska3 signal (green). The images to the right are enlarged images of kinetochores with Ska3 signal in green and CREST signal in red. (**B**) The Ska3 signal at kinetochores was quantified and normalized to the CREST signal. For each condition, at least 110 kinetochores were analyzed in 11 different cells. The average and standard deviation is shown.

Recruitment of the Ska complex to kinetochores

The Ska1 protein was originally identified in a mass spectrometry screen of the mitotic spindle which lead to the identification of the Ska complex composed of Ska1, Ska2 and Ska3 (Guimaraes and Deluca, 2009). In vitro the reconstituted Ska complex has a similar affinity to microtubules as the reconstituted KMN network and also appears to interact with the acidic C-terminus of microtubules (Welburn et al., 2009). While incomplete removal of Ska components leads to a delay in the metaphase to anaphase transition (Gaitanos et al., 2009; Hanisch et al., 2006; Welburn et al., 2009), the complete removal of Ska complex activity results in a very similar phenotype as Ndc80 depletion with a failure in chromosome congression and absence of cold stable microtubules (Gaitanos et al., 2009; Welburn et al., 2009). Thus

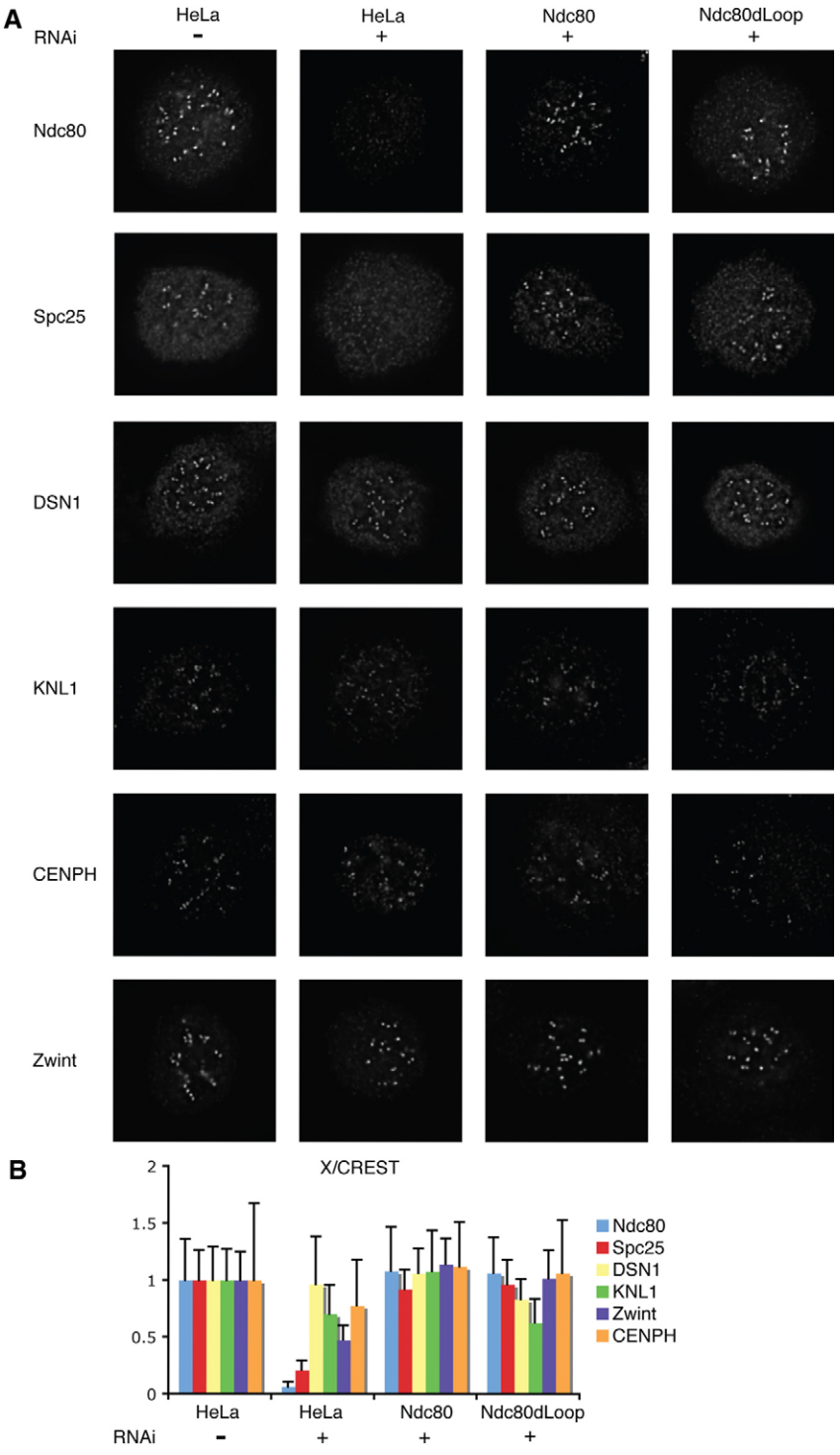

Fig. 6. Incorporation of the KMN network components in Ndc80dLoop. (**A**) Immunofluorescence analysis of kinetochore components following depletion of endogenous Ndc80 and rescue with Ndc80 or Ndc80dLoop. The cells were kept in prometaphase by nocodazole treatment. Cells were stained for the protein indicated on the left and CREST. (**B**) The signal at kinetochores for Ndc80, Spc25, DSN1, KNL1, Zwint and CENP-H was quantified on at least 60 kinetochores in six different cells. The signal was normalized to the CREST signal and the average and standard deviation is shown.

the Ska complex has an essential role in establishing kinetochore–microtubule interactions.

The recruitment of the Ska complex to kinetochores depends on the Ndc80 complex and is stimulated by microtubule binding to kinetochores (Hanisch et al., 2006). Several lines of evidence presented here supports a specific role of the Ndc80 loop in recruiting the Ska complex to kinetochores. Firstly, the Ska components had background ratios in our mass spectrometry samples of Ndc80dLoop even though other transient kinetochore proteins such as Bub1 and BubR1 are still present. Secondly, quantitative immunofluorescence reveals a defect in the recruitment of the Ska complex in Ndc80 loop mutants but not in the Ndc80 K166E mutant that is also unable to bind microtubules and make end-on attachments. Thirdly, the phenotype of the Ndc80 loop mutants described here resembles the phenotype of complete Ska complex depletion. We have also analyzed Ska1 localization

following KNL1 depletion but this only leads to a minor decrease in Ska1 levels indicating that the Ndc80 complex is providing the major interaction site for the Ska complex.

A direct interaction between the Ndc80 complex and the Ska complex has not been observed [see discussion in Hanisch et al. (Hanisch et al., 2006)] and potentially another protein bridges the interaction between the two complexes or post translational modifications are required for them to bind. Currently we cannot rule out that Ndc80 loop mutants affects the orientation and interactions within the KMN network and that the Ska complex has multiple interactions within the KMN network that has to be positioned correctly for productive binding to occur. Understanding how the interaction between the Ndc80 complex and the Ska complex and their activities are regulated will be crucial goals for the future but the function of the Ndc80 loop region described here is an important step forward.

Materials and Methods

Cloning and cell lines

Ndc80 was amplified with the primers 5′-GTACAAGCTTACCATGAAGCGC-AGTTCAG-3′ and 5′-GTACGCGGCCGCGCTTCTTCAGAAGACTTAATTAG-3′ and cloned into the HindIII and the NotI site of pcDNA5/FRT/TO Venus. The Ndc80 was made insensitive to the RNAi oligo (5′-GAGUAGAACUAGA-AUGUGA-3′) by introducing silent mutations in Ndc80 with quick change PCR using the following primers: 5′-GGAAATTGCTAGAGTGGAGCTTGAGTG-TGAAACAATAAAA-3′ and its reverse complement. The loop region was removed from pcDNA5/FRT/TO Ndc80 Venus and pGEX 6P 2RBS Ndc80/Nuf2 (a gift from Andrea Musacchio) by performing quick change PCR with 5′-GCTAGAAAATTAAAACTTATTCCTGTCAAATACAGGGCTCAAG-3′ and its reverse complement. To reverse the loop sequence in Ndc80 a two step PCR protocol was used. All constructs were verified by sequencing.

Generation of stable HeLa/FRT/TRex cell lines expressing inducible Ndc80 constructs were done as described previously (Nilsson et al., 2008).

Protein expression and tubulin binding

Expression and purification of Ndc80 complexes was done as described by Ciferri et al. (Ciferri et al., 2005). Ndc80 protein stocks were kept in 50 mM Tris-HCl, 600 mM NaCl, 1 mM DTT, 1 EDTA pH 7.6 at −20℃.

Tubulin was diluted in BRB80 buffer (80 mM Pipes/KOH pH 6.8, 1 mM $MgCl_2$, 1 mM EGTA) and stabilized with 100 nM Taxol and 1 mM GDPNP as described by the supplier (Cytoskeleton, Inc.). Ndc80 complexes were diluted to 1 μM in BRB80 buffer with 10% glycerol and 5 μl of this was mixed with 20 μl tubulin suspension. After incubation for 5 min. at room temperature the binding reaction was placed on top of a 100 μl glycerol cushion (BRB80 with 50% glycerol and 100 nM Taxol and 1 mM GDPNP) and centrifuged for 17 min at 36,000 ***g***. The supernatant and cushion were removed and the pellet was resuspended and analyzed by SDS-PAGE.

EM analysis

Purified protein was exchanged into a buffer containing 50 mM Tris pH 7.5, 100 mM NaCl at 20 μg/ml on a Superose 6 column and directly used to prepare grids. Protein complexes were applied to glow-discharged, carbon-coated grids, stained with 2% (w/v) uranyl acetate and visualized using a JEOL 1010 microscope (JEOL, Japan) operating at 80 kV. Image analysis was carried out using ImageJ (NIH).

Immunofluorescence and antibodies

Cells growing on coverslips were pre-extracted with 0.5% Triton X-100 in PHEM buffer (60 mM PIPES, 25 mM HEPES, pH 6.9, 10 mM EGTA, 4 mM $MgSO_4$) for 5 min before fixation by 4% paraformaldehyde in PHEM buffer for 20 min at 37℃. For microtubule stability assay, cells were incubated on ice for 15 min before pre-extraction and fixation. The antibodies used for cell staining include Ndc80 (Abcam, ab3613, 1:200), CREST (Antibodies Inc., 15-235-0001, 1:400), tubulin (Abcam, ab6160, 1:250), BubR1 (Bethyl, A300-386A, 1:400), Mad1 (Sigma, M8069, 1:200), Spc25 (gift from Todd Stukenberg, 1:500), CENP-H (gift from Patrick Meraldi, 1:4000), Nuf2 (Abcam, ab17058, 1:300), Ska1 (gift from Erich Nigg, 1:500), Ska3 (gift from Erich Nigg, 1:500), GFP (Abcam, ab290, 1:400) and Zwint (Bethyl, A300-781A, 1:200). Fluorescent secondary antibodies were Alexa Fluor dyes (Invitrogen, 1:1000). Images were collected using a 100× objective on a Deltavision microscope (Applied Precision, Washington, USA) with 200 nm between each stack. Protein intensity on kinetochores was quantified by drawing a circle closely along the rod-like CREST staining and encompassing the outer kinetochore protein of interest on both kinetochores of a pair. The intensity values from all stacks were calculated and the intensity from the three continuous peak stacks were subtracted the background from neighboring areas and averaged. All the averaged intensity was normalized against the CREST fluorescent intensity.

Ndc80 RNAi and rescue

HeLa stable cell lines were cultured in DMEM medium (Invitrogen) supplemented with 10% fetal bovine serum, penicillin streptomycin, hygromycin B and blasticidin (Invitrogen). Cells were synchronized by 2 mM thymidine (Sigma) for 24 hr before transfection with 50 nM Ndc80 or luciferase RNAi oligo (Sigma; 5′-CGUACGCGGAAUACUUCGA-3′) by Lipofectamine RNAiMAX Transfection Reagent (Invitrogen). The expression of wild type or mutant Ndc80 constructs was induced immediately after RNAi treatment. 12 hr after RNAi treatment the cells were arrested with aphidicolin (Sigma) for 24 hr. After release from the aphidicolin block [into medium containing 200 ng/ml nocodazole (Sigma) for KMN network component staining or into fresh medium for the mitotic spindle or Ska complex staining], the cells were fixed and stained with the specified antibodies.

Live cell imaging

Cells grown on eight-well slides (Ibidi) were washed once with PBS before being cultured in L-15 medium supplemented with 10% fetal bovine serum (Invitrogen). The slide was mounted onto a Deltavision microscope for live cell imaging. A 40× oil-immersion objective was used and the DIC and YFP channels were recorded for 12 hrs at 4–10 min intervals. ImageJ (NIH) and Softworx were used to analyze the data.

Immunoprecipitation

Cells expressing wild type or mutant Ndc80 were lysed in lysis buffer (10 mM Tris-HCl pH 7.5, 150 mM NaCl, 0.5 mM EDTA and 0.5% NP40). GFP–Trap (ChromoTek) beads were applied to the cleared cell lysate and incubated for 10 min at room temperature or 1 h at 4℃. Protein complexes captured by the GFP-binder beads were eluted in 2× SDS sample buffer and boiled for 10 min at 95℃.

SILAC labeling

Generally SILAC DMEM media without arginine and lysine (PAA) was supplemented with 10% dialyzed fetal bovine serum (PAA), Penicillin Streptomycin and Glutamax (Invitrogen) and isotope labeled arginine and lysine. L-lysine/HCl and L-arginine/HCl (Sigma) were used for light culture. L-lysine/2HCl (4,4,5,5-D4, 98%) and L-arginine (U-13C6, 99%) (Cambridge Isotope Laboratories) were used for medium culture while L-lysine/2HCl (U-13C6, 99%; U-15N2, 99%) and L-arginine/HCl (U-13C6, 99%; U-15N4, 99%; Cambridge Isotope Laboratories) were for heavy culture. Cells seeded in SILAC medium were cultured for at least five divisions before harvest. Induction of the wild-type or mutant Ndc80 constructs was performed 48 hrs before harvesting. Immunoprecipitation was performed as described above from cell lysate with equal amounts of protein.

Mass spectrometry analysis

The eluate from the beads were reduced and alkylated and loaded onto an SDS–PAGE gel. The lane was cut into 10 pieces and subjected to in-gel tryptic digestion and subsequent sample desalting and concentration, as described previously (Shevchenko et al., 2006). The resulting peptide mixture was analyzed by nano-HPLC–MS/MS using an easy-nLC nanoflow system (Thermo Scientific, Odense, Denmark) connected to an LTQ-Orbitrap Velos mass spectrometer (Thermo Scientific, Bremen, Germany) through a nano-electrospray ion source. The column length was 150 mm with 75-μm inner diameter, and packed in-house with 3-μm C_{18} beads (Reprosil-AQ Pur, Dr. Maisch). Each sample was analyzed using a 120-min gradient from 5 to 35% acetonitrile in 0.5% acetic acid. The mass spectrometer was run in a data dependent mode choosing the ten most intense peaks for HCD fragmentation and measurement in the orbitrap with dynamic exclusion enabled. Fullscans were acquired at a resolution of 30,000 and a target values set to 1e6 with a maximum injection time of 500 ms. Fragment scans were measured at 35% collision energy at a resolution of 7500 with a set target value of 5e4 and a maximum injection time of 250 μms. Lock mass was enabled during the run (Olsen et al., 2005).

Data analysis was performed in the MaxQuant environment version 1.2.0.24 using the Andromeda search engine. The database searched was the Human International Protein Index version 3.68 (EBI, United Kingdom) concatenated with a list of commonly observed background contaminants. For the search oxidation of methionine, protein N-terminal acetylation, and N-terminal glutamine to pyroglutamate were specified as variable modifications and carbamidomethyl of cysteine was set as fixed modification. The FDR rate was set at 1% according to the decoy database search strategy (Elias and Gygi, 2007).

Acknowledgements

We thank Erich Nigg, Patrick Meraldi, Arshad Desai, Andrea Musacchio and Todd Stukenberg for providing antibodies and reagents and Stephen Taylor for providing the HeLa/FRT/TRex cell line. The authors have no conflicts of interest.

Funding

This work was supported by the Danish Research Council [grant number 11-105247 to G.Z.]; the Lundbeck Foundation [grant number R28-A1977 to J.N.]; the Danish Cancer Society [grant number R2-A101-09-S2 to J.N.]; Cancer Research UK [grant number xxxx to M.S.]; and the Novo Nordisk Foundation [grant number xxxx to J.V.O.].

Supplementary material available online at
http://jcs.biologists.org/lookup/suppl/doi:10.1242/jcs.104208/-/DC1

References

Akiyoshi, B., Nelson, C. R., Ranish, J. A. and Biggins, S. (2009). Analysis of Ipl1-mediated phosphorylation of the Ndc80 kinetochore protein in Saccharomyces cerevisiae. *Genetics* **183**, 1591-1595.

Alushin, G. M., Ramey, V. H., Pasqualato, S., Ball, D. A., Grigorieff, N., Musacchio, A. and Nogales, E. (2010). The Ndc80 kinetochore complex forms oligomeric arrays along microtubules. *Nature* **467**, 805-810.

Barisic, M., Sohm, B., Mikolcevic, P., Wandke, C., Rauch, V., Ringer, T., Hess, M., Bonn, G. and Geley, S. (2010). Spindly/CCDC99 is required for efficient chromosome congression and mitotic checkpoint regulation. *Mol. Biol. Cell* **21**, 1968-1981.

Chan, Y. W., Fava, L. L., Uldschmid, A., Schmitz, M. H., Gerlich, D. W., Nigg, E. A. and Santamaria, A. (2009). Mitotic control of kinetochore-associated dynein and spindle orientation by human Spindly. *J. Cell Biol.* **185**, 859-874.

Cheeseman, I. M. and Desai, A. (2008). Molecular architecture of the kinetochore-microtubule interface. *Nat. Rev. Mol. Cell Biol.* **9**, 33-46.

Cheeseman, I. M., Chappie, J. S., Wilson-Kubalek, E. M. and Desai, A. (2006). The conserved KMN network constitutes the core microtubule-binding site of the kinetochore. *Cell* **127**, 983-997.

Ciferri, C., De Luca, J., Monzani, S., Ferrari, K. J., Ristic, D., Wyman, C., Stark, H., Kilmartin, J., Salmon, E. D. and Musacchio, A. (2005). Architecture of the human ndc80-hec1 complex, a critical constituent of the outer kinetochore. *J. Biol. Chem.* **280**, 29088-29095.

Ciferri, C., Pasqualato, S., Screpanti, E., Varetti, G., Santaguida, S., Dos Reis, G., Maiolica, A., Polka, J., De Luca, J. G., De Wulf, P. et al. (2008). Implications for kinetochore-microtubule attachment from the structure of an engineered Ndc80 complex. *Cell* **133**, 427-439.

Daum, J. R., Wren, J. D., Daniel, J. J., Sivakumar, S., McAvoy, J. N., Potapova, T. A. and Gorbsky, G. J. (2009). Ska3 is required for spindle checkpoint silencing and the maintenance of chromosome cohesion in mitosis. *Curr. Biol.* **19**, 1467-1472.

DeLuca, J. G., Moree, B., Hickey, J. M., Kilmartin, J. V. and Salmon, E. D. (2002). hNuf2 inhibition blocks stable kinetochore-microtubule attachment and induces mitotic cell death in HeLa cells. *J. Cell Biol.* **159**, 549-555.

DeLuca, J. G., Dong, Y., Hergert, P., Strauss, J., Hickey, J. M., Salmon, E. D. and McEwen, B. F. (2005). Hec1 and nuf2 are core components of the kinetochore outer plate essential for organizing microtubule attachment sites. *Mol. Biol. Cell* **16**, 519-531.

DeLuca, J. G., Gall, W. E., Ciferri, C., Cimini, D., Musacchio, A. and Salmon, E. D. (2006). Kinetochore microtubule dynamics and attachment stability are regulated by Hec1. *Cell* **127**, 969-982.

Elias, J. E. and Gygi, S. P. (2007). Target-decoy search strategy for increased confidence in large-scale protein identifications by mass spectrometry. *Nat. Methods* **4**, 207-214.

Gaitanos, T. N., Santamaria, A., Jeyaprakash, A. A., Wang, B., Conti, E. and Nigg, E. A. (2009). Stable kinetochore-microtubule interactions depend on the Ska complex and its new component Ska3/C13Orf3. *EMBO J.* **28**, 1442-1452.

Guimaraes, G. J. and Deluca, J. G. (2009). Connecting with Ska, a key complex at the kinetochore-microtubule interface. *EMBO J.* **28**, 1375-1377.

Guimaraes, G. J., Dong, Y., McEwen, B. F. and Deluca, J. G. (2008). Kinetochore-microtubule attachment relies on the disordered N-terminal tail domain of Hec1. *Curr. Biol.* **18**, 1778-1784.

Hanisch, A., Silljé, H. H. and Nigg, E. A. (2006). Timely anaphase onset requires a novel spindle and kinetochore complex comprising Ska1 and Ska2. *EMBO J.* **25**, 5504-5515.

Hsu, K. S. and Toda, T. (2011). Ndc80 internal loop interacts with Dis1/TOG to ensure proper kinetochore-spindle attachment in fission yeast. *Curr. Biol.* **21**, 214-220.

Karess, R. (2005). Rod-Zw10-Zwilch: a key player in the spindle checkpoint. *Trends Cell Biol.* **15**, 386-392.

Lampson, M. A. and Kapoor, T. M. (2005). The human mitotic checkpoint protein BubR1 regulates chromosome-spindle attachments. *Nat. Cell Biol.* **7**, 93-98.

Lupas, A., Van Dyke, M. and Stock, J. (1991). Predicting coiled coils from protein sequences. *Science* **252**, 1162-1164.

Martin-Lluesma, S., Stucke, V. M. and Nigg, E. A. (2002). Role of Hec1 in spindle checkpoint signaling and kinetochore recruitment of Mad1/Mad2. *Science* **297**, 2267-2270.

Maskell, D. P., Hu, X. W. and Singleton, M. R. (2010). Molecular architecture and assembly of the yeast kinetochore MIND complex. *J. Cell Biol.* **190**, 823-834.

Maure, J. F., Komoto, S., Oku, Y., Mino, A., Pasqualato, S., Natsume, K., Clayton, L., Musacchio, A. and Tanaka, T. U. (2011). The Ndc80 loop region facilitates formation of kinetochore attachment to the dynamic microtubule plus end. *Curr. Biol.* **21**, 207-213.

Meraldi, P. and Sorger, P. K. (2005). A dual role for Bub1 in the spindle checkpoint and chromosome congression. *EMBO J.* **24**, 1621-1633.

Meraldi, P., Draviam, V. M. and Sorger, P. K. (2004). Timing and checkpoints in the regulation of mitotic progression. *Dev. Cell* **7**, 45-60.

Miller, S. A., Johnson, M. L. and Stukenberg, P. T. (2008). Kinetochore attachments require an interaction between unstructured tails on microtubules and Ndc80(Hec1). *Curr. Biol.* **18**, 1785-1791.

Nilsson, J., Yekezare, M., Minshull, J. and Pines, J. (2008). The APC/C maintains the spindle assembly checkpoint by targeting Cdc20 for destruction. *Nat. Cell Biol.* **10**, 1411-1420.

Olsen, J. V., de Godoy, L. M., Li, G., Macek, B., Mortensen, P., Pesch, R., Makarov, A., Lange, O., Horning, S. and Mann, M. (2005). Parts per million mass accuracy on an Orbitrap mass spectrometer via lock mass injection into a C-trap. *Mol. Cell. Proteomics* **4**, 2010-2021.

Ong, S. E. and Mann, M. (2006). A practical recipe for stable isotope labeling by amino acids in cell culture (SILAC). *Nat. Protoc.* **1**, 2650-2660.

Ong, S. E., Blagoev, B., Kratchmarova, I., Kristensen, D. B., Steen, H., Pandey, A. and Mann, M. (2002). Stable isotope labeling by amino acids in cell culture, SILAC, as a simple and accurate approach to expression proteomics. *Mol. Cell. Proteomics* **1**, 376-386.

Petrovic, A., Pasqualato, S., Dube, P., Krenn, V., Santaguida, S., Cittaro, D., Monzani, S., Massimiliano, L., Keller, J., Tarricone, A. et al. (2010). The MIS12 complex is a protein interaction hub for outer kinetochore assembly. *J. Cell Biol.* **190**, 835-852.

Powers, A. F., Franck, A. D., Gestaut, D. R., Cooper, J., Gracyzk, B., Wei, R. R., Wordeman, L., Davis, T. N. and Asbury, C. L. (2009). The Ndc80 kinetochore complex forms load-bearing attachments to dynamic microtubule tips via biased diffusion. *Cell* **136**, 865-875.

Rieder, C. L. (1981). The structure of the cold-stable kinetochore fiber in metaphase PtK1 cells. *Chromosoma* **84**, 145-158.

Rothbauer, U., Zolghadr, K., Muyldermans, S., Schepers, A., Cardoso, M. C. and Leonhardt, H. (2008). A versatile nanotrap for biochemical and functional studies with fluorescent fusion proteins. *Mol. Cell. Proteomics* **7**, 282-289.

Salmon, E. D. and Begg, D. A. (1980). Functional implications of cold-stable microtubules in kinetochore fibers of insect spermatocytes during anaphase. *J. Cell Biol.* **85**, 853-865.

Schmidt, J. C. and Cheeseman, I. M. (2011). Chromosome segregation: keeping kinetochores in the loop. *Curr. Biol.* **21**, R110-R112.

Schmidt, J. C., Kiyomitsu, T., Hori, T., Backer, C. B., Fukagawa, T. and Cheeseman, I. M. (2010). Aurora B kinase controls the targeting of the Astrin-SKAP complex to bioriented kinetochores. *J. Cell Biol.* **191**, 269-280.

Shevchenko, A., Tomas, H., Havlis, J., Olsen, J. V. and Mann, M. (2006). In-gel digestion for mass spectrometric characterization of proteins and proteomes. *Nat. Protoc.* **1**, 2856-2860.

Sundin, L. J., Guimaraes, G. J. and Deluca, J. G. (2011). The NDC80 complex proteins Nuf2 and Hec1 make distinct contributions to kinetochore-microtubule attachment in mitosis. *Mol. Biol. Cell* **22**, 759-768.

Theis, M., Slabicki, M., Junqueira, M., Paszkowski-Rogacz, M., Sontheimer, J., Kittler, R., Heninger, A. K., Glatter, T., Kruusmaa, K., Poser, I. et al. (2009). Comparative profiling identifies C13orf3 as a component of the Ska complex required for mammalian cell division. *EMBO J.* **28**, 1453-1465.

Tooley, J. G., Miller, S. A. and Stukenberg, P. T. (2011). The Ndc80 complex uses a tripartite attachment point to couple microtubule depolymerization to chromosome movement. *Mol. Biol. Cell* **22**, 1217-1226.

Wan, X., O'Quinn, R. P., Pierce, H. L., Joglekar, A. P., Gall, W. E., DeLuca, J. G., Carroll, C. W., Liu, S. T., Yen, T. J., McEwen, B. F. et al. (2009). Protein architecture of the human kinetochore microtubule attachment site. *Cell* **137**, 672-684.

Wang, H. W., Long, S., Ciferri, C., Westermann, S., Drubin, D., Barnes, G. and Nogales, E. (2008). Architecture and flexibility of the yeast Ndc80 kinetochore complex. *J. Mol. Biol.* **383**, 894-903.

Wei, R. R., Sorger, P. K. and Harrison, S. C. (2005). Molecular organization of the Ndc80 complex, an essential kinetochore component. *Proc. Natl. Acad. Sci. USA* **102**, 5363-5367.

Welburn, J. P. and Cheeseman, I. M. (2008). Toward a molecular structure of the eukaryotic kinetochore. *Dev. Cell* **15**, 645-655.

Welburn, J. P., Grishchuk, E. L., Backer, C. B., Wilson-Kubalek, E. M., Yates, J. R., 3rd and Cheeseman, I. M. (2009). The human kinetochore Ska1 complex facilitates microtubule depolymerization-coupled motility. *Dev. Cell* **16**, 374-385.

Welburn, J. P., Vleugel, M., Liu, D., Yates, J. R., 3rd, Lampson, M. A., Fukagawa, T. and Cheeseman, I. M. (2010). Aurora B phosphorylates spatially distinct targets to differentially regulate the kinetochore-microtubule interface. *Mol. Cell* **38**, 383-392.

Whyte, J., Bader, J. R., Tauhata, S. B., Raycroft, M., Hornick, J., Pfister, K. K., Lane, W. S., Chan, G. K., Hinchcliffe, E. H., Vaughan, P. S. et al. (2008). Phosphorylation regulates targeting of cytoplasmic dynein to kinetochores during mitosis. *J. Cell Biol.* **183**, 819-834.

Wigge, P. A. and Kilmartin, J. V. (2001). The Ndc80p complex from Saccharomyces cerevisiae contains conserved centromere components and has a function in chromosome segregation. *J. Cell Biol.* **152**, 349-360.

Yen, T. J., Compton, D. A., Wise, D., Zinkowski, R. P., Brinkley, B. R., Earnshaw, W. C. and Cleveland, D. W. (1991). CENP-E, a novel human centromere-associated protein required for progression from metaphase to anaphase. *EMBO J.* **10**, 1245-1254.